

Little-Parks effect in single nanoscale $\text{YBa}_2\text{Cu}_3\text{O}_{6+x}$ rings

Franco Carillo,¹ Gianpaolo Papari,² Daniela Stornaiuolo,^{2,3} Detlef Born,¹ Domenico Montemurro,^{2,1}
Pasqualantonio Pingue,¹ Fabio Beltram,¹ and Francesco Tafuri^{1,3}

¹*NEST, CNR-INFM and Scuola Normale Superiore, Piazza San Silvestro 12, I-56127 Pisa, Italy*

²*Dipartimento Scienze Fisiche and SPIN INFM-CNR, Università di Napoli Federico II, Napoli, Italy*

³*Dipartimento di Ingegneria dell'Informazione and SPIN INFM-CNR, Seconda Università di Napoli, Aversa, I-81031 Caserta, Italy*

(Received 3 November 2009; revised manuscript received 7 January 2010; published 10 February 2010)

The properties of single submicron high-temperature superconductor (HTS) rings are investigated. The Little-Parks effect is observed and is accompanied by an anomalous behavior of the magnetic dependence of the resistance, which we ascribe to nonuniform vorticity (superfluid angular momentum) within the ring arms. This effect is linked to the peculiar HTS relationship between the values of the coherence length and the London penetration depth.

DOI: [10.1103/PhysRevB.81.054505](https://doi.org/10.1103/PhysRevB.81.054505)

PACS number(s): 74.25.Jb, 74.25.Uv, 74.72.-h

I. INTRODUCTION

Rings and, more generally, multiply connected systems are powerful tools to investigate purely quantum phenomena such as gauge invariance and quantum interference in superconducting¹ and normal-state systems.² In particular, Aharonov-Bohm³ and Little-Parks (LP)^{4–6} effects represent paradigmatic examples of coherent quantum phenomena occurring in simple loops for the case of single particles and of the collective superconducting state, respectively. In the case of mesoscopic structures made of low critical-temperature superconductors (LTS), devices with characteristic dimensions comparable or lower than the coherence length (ξ_0) are today accessible and allowed a number of exciting experiments on superconductivity at the nanoscale.^{5–8} Similar scaling regimes cannot be achieved in the case of high critical-temperature superconductors (HTS) because of the very small value of the coherence length in perfectly doped HTS ($\xi_0 \approx 1.5$ nm). Nevertheless currently available linewidths of the order of few tens of nanometers in HTS open the way to the experimental study of structures with length scales comparable or smaller than the London penetration length (λ_L), or the typical grain size in epitaxial thin films, or the possible stripe charge-order correlation length (40 nm).^{9–11} Indeed, rings on the deep submicron scale are expected to shed light on various issues related to the HTS pairing mechanism^{9–13} and to the peculiar vortex states produced by the d -wave order-parameter symmetry.^{12–18} Also, it was recently claimed that since in a d -wave system robust superconductivity along specific directions can coexist with low-energy quasiparticles, a crossover between the typical $h/2e$ superconducting and h/e quasiparticle flux periodicity^{12,14,15,18} should be observed in mesoscopic loops of length scales even larger than ξ_0 .

In the present work we report $h/2e$ Little-Parks flux periodicity in nanoscale HTS rings. When compared with analogous experiments performed on LTS loops with a similar ratio between internal and external radii^{19,20} or on arrays of micron-sized HTS holes,²¹ our results provide clear evidence of a nonuniform vorticity of the order parameter in the rings. We shall discuss this “concentric-vortex” structure which results from the very short coherence length and a

London penetration depth λ_L which is, in turn, larger than the width of the ring arms. It is worth mentioning that since ξ is of the order of few nanometers, our findings are relevant even to ring radii smaller than the ones studied here, down to the nanometer scale.

Isothermal measurements of resistance vs magnetic field [$R(H)$] of submicron rings patterned on $\text{YBa}_2\text{Cu}_3\text{O}_{6+x}$ (YBCO) c -axis thin films were performed on several different samples. By measuring $R(H)$ at temperatures close to the critical temperature (T_c) in a mesoscopic loop^{5,6} it is possible to determine its normal-to-superconducting phase boundary, in full analogy with the experiments reported by Little and Parks⁴ on cylinders to evidence fluxoid quantization.¹ As explicitly shown in Ref. 5, in structures of characteristic size comparable to ξ , the phase boundary strongly depends on the specific shape of the structure.

In HTS the detection of T_c vs H oscillations can be very challenging since their amplitude (ΔT_c) is expected to scale with $(\xi_0/r)^2$. In one of the few successful attempts a maximum $\Delta T_c \approx 40$ mK was observed in a 50×50 array of $1 \mu\text{m} \times 1 \mu\text{m}$ holes in YBCO c -axis films.²¹ In our rings with a radius of a few hundred nanometers, ΔT_c oscillations show an amplitude of about 500 mK on single YBCO loops. In our single-ring configuration higher spurious harmonics in the magnetoresistance are not introduced as opposed to arrays of rings. In these last systems the magnetoresistance is the convolution of the fundamental period, which corresponds to a flux quantum in a single cell, but also of all the periods corresponding to a flux quantum in two or several cells of the array. Consequently in an array, it is difficult to distinguish these contributions from intrinsic effects with integer fractions of $h/2e$ in a single loop.²²

II. EXPERIMENT

We shall report on measurements performed on four YBCO rings having nominally identical shape (internal radius $r_i = 200$ nm, external radius $r_o = 500$ nm) but different critical temperatures ranging from 74 to 19 K. These samples allow us to cover a large part of the superconducting phase diagram in the underdoped regime. At lower T_c interference due to quasiparticles is expected to play a larger role also

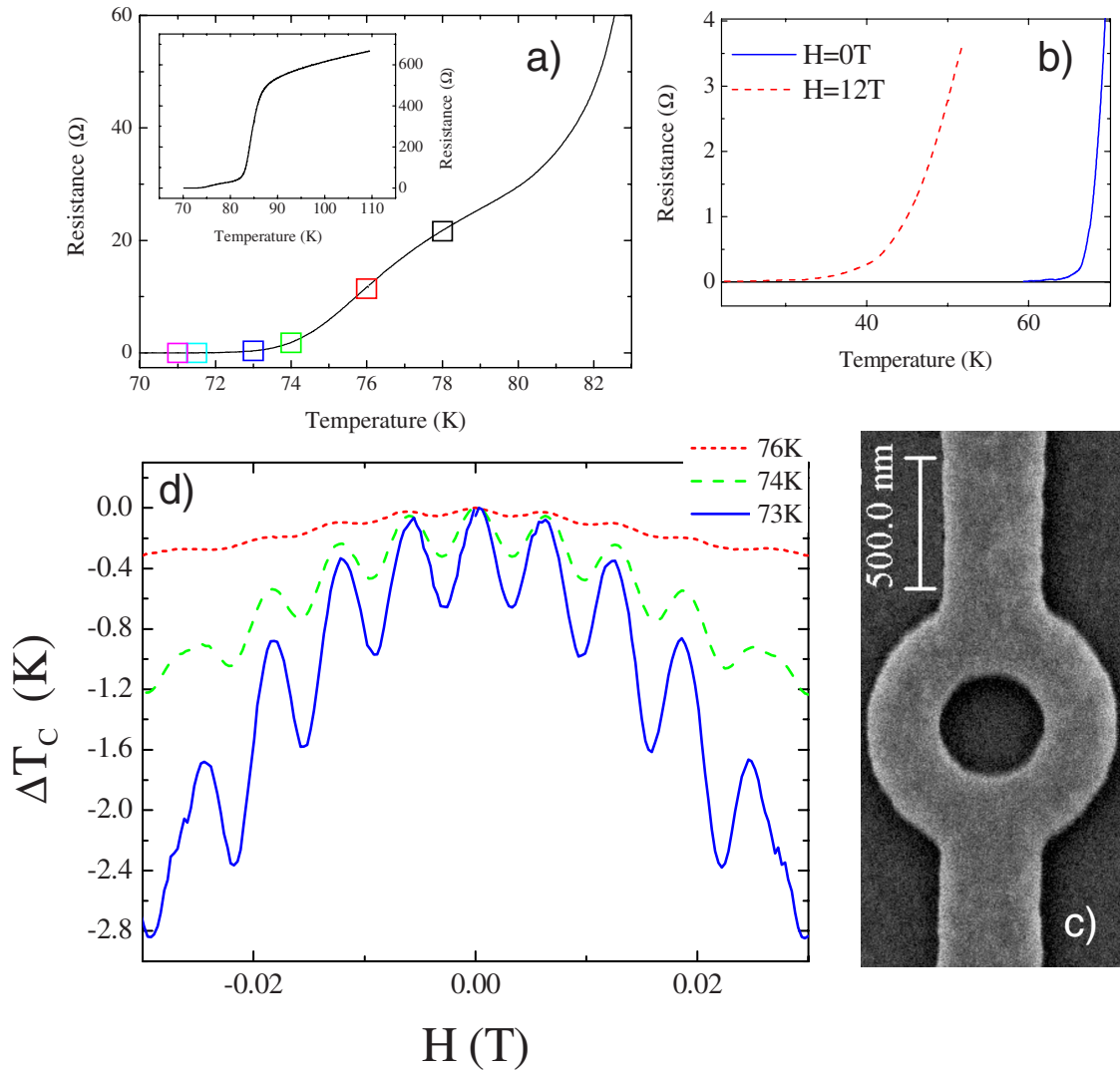


FIG. 1. (Color online) (a) Detail of the resistance vs temperature curve in proximity of the critical temperature T_c and on a larger scale (inset) for ring D1. In (b) $R(T)$ curves measured at $H=0$ T and $H=12$ T, in an underdoped ring nominally identical to D1, are reported in proximity of T_c . In (c) scanning electron micrograph of ring (D1). In (d) oscillations of ΔT_c derived by measurements of the magnetoconductance (see text) on the same device, are shown at different temperatures, providing evidence of Little-Parks effect.

owing to the longer thermal length. To the best of our knowledge single-particle Aharonov-Bohm interference was recorded up to the maximum temperature of 20 K on semiconductor rings with similar size.²³

We fabricated our nanostructures starting from 50-nm-thick (001)-oriented YBCO films grown on yttrium stabilized zirconia (YSZ) and SrTiO₃ substrates. The typical value of the surface roughness was lower than 3 nm. A 20 nm gold layer was deposited *in situ* to protect YBCO films during all following fabrication steps. In order to fabricate the nanostructures we deposited on top of the YBCO/Au bilayer a 50-nm-thick Ti mask that was patterned by electron-beam lithography and lift-off. The exposed YBCO/Au bilayer was etched by ion-beam etching (IBE) while the sample was cooled down at -140 °C in order to minimize oxygen loss from YBCO films. Subsequently the Ti mask was removed by a highly diluted HF solution (1:20) and the gold layer by a low-energy IBE. Figure 1(c) reports a scanning electron microscope picture of one of the nanostructures (D1).

The critical temperature of a device patterned using this procedure depends on the linewidth and on etching conditions. The more energetic is the dry etching and the smaller are the linewidths, the more depressed are the superconducting properties of nanostructures. This makes it possible to tune the ring doping level. We measured four rings, with an average radius of 350 nm and branch width ranging from 270 to 300nm. For all devices the transition temperature of the larger YBCO areas, i.e., wiring and pads, corresponds to that of the unpatterned film (86 K). All samples showed the expected tail in the resistance vs temperature curve associated with the superconducting transition of the submicron part of the device [see Fig. 1(a) for device D1]. In Fig. 1(b) we show $R(T)$ curves at zero magnetic field and at 12 T close to T_c for a similar ring with a lower doping. In experiments on single crystals and thin films, the exponential growth of the resistivity in an extended temperature range above the zero resistance state²⁴ has been associated with a vortex-liquid state (VLS) (Refs. 25 and 26) in the complex magnetic

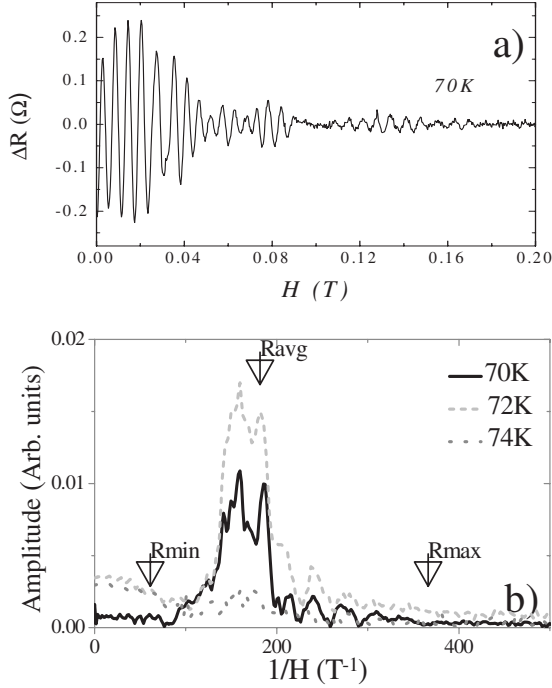


FIG. 2. (a) Resistance oscillations of a ring with $R_{\max}=445$ nm and $R_{\min}=205$ nm (D2). (b) FFT of $R(H)$ data taken at three temperatures. Black arrows indicate the frequencies corresponding to a single-flux quantum in a ring with radius R_{\min} , R_{avg} , and R_{\max} , respectively.

phase diagram. Even if the conditions of occurrence of VLS in HTS nanostructures go beyond the aims of the present work, the $R(T)$ curve, measured at 12 T (which is the maximum field we can apply in our setup) and shown in Fig. 1(b) close to T_c , gives relevant indications. Its characteristic shape accompanied by a reduction in T_c of about 25 K (on the order of 40% of the original T_c), suggests a mechanism based on VLS for the onset of resistance also in our nanostructures, where the width is comparable to the London penetration depth and much smaller than the Pearl length.

Measurements were performed in liquid helium using a variable-temperature probe. Thermal stability was ensured by a heater connected to a proportional-integral-derivative controller. Current and voltage leads were filtered by RC filters at room temperature. A second filtering stage consisted of RC plus copper-powder filters thermally anchored at 4.2 K. Shielding from spurious external magnetic fields was provided by a combination of nested cryoperm, Pb, and Nb foils all placed in the measurement Dewar and immersed in liquid He. For all the measurements reported here we consider the differential resistance ($dR=dV/dI$) at zero bias as function of temperature and magnetic field. dR is measured by biasing the device with a small ac current (typically 300 nA) at about 11 Hz and detecting the corresponding ac voltage with a lock-in amplifier.

Following the standard procedure of LP experiments on LTS samples, we measured the magnetoconductance at several temperatures above T_{c0} defined as the temperature at which the voltage drop is zero within the error of the instrument. From the magnetoconductance and the $R(T)$ curves we

calculated $\Delta T_c = \Delta R (dR/dT)^{-1}$. In all devices ΔT_c oscillations show a periodicity $h/2e$ as function of the flux enclosed by the ring average area $A = \pi r_{avg}^2$, as shown in Fig. 1(c) for D1. For our geometry this area matches with theoretical predictions for annulus of arbitrary r_i/r_o ratio.²⁷ Consistently with similar measurements on the LP effect,^{4-6,21,28} the periodic dependence of ΔT_c is superimposed on a parabolic background determined by the contribution to magnetoconductance of single wires.²⁸ The amplitude of T_c oscillations depended on the temperature at which the $R(H)$ was measured. The maximum value of $\Delta T_c = 600$ mK was recorded at 73 K, and far exceeds the value predicted by theory for clean superconductors: $\Delta T_c = 0.14 T_c (\xi_0/r)^2 \sim 1$ mK, assuming a zero-temperature coherence length $\xi_0 = 1.5$ nm. This large discrepancy is consistent with previous experiments on HTS (Ref. 21) and conventional systems²⁸ and has been linked to a smooth $R(T)$ since early times.²⁸ Current leads connected to the rings are quite larger than the arms of the ring [an example is given in Fig. 1(c)]. This has guaranteed that for the presented experiments we have never been in a situation for which the leads were normal and the ring superconducting, differently from other configurations studied in literature (Ref. 29). The results in Ref. 29 suggest that in our experiment possible more subtle processes induced by nonequilibrium effects produced by normal leads are negligible with respect to the shielding current phenomena in the loop (i.e., Little-Parks effect).

The magnetic field behavior of severely underdoped rings with T_c 24 and 19 K is substantially identical to those with larger doping. In particular, we have found that, within our sensitivity and noise level, the oscillatory signal of magnetoresistance quickly disappears above T_c (typically in a temperature range $\Delta T/T_c$ less than 5%). The absence of an oscillatory response does not necessarily argue against the scenario of Cooper pairs surviving at temperatures larger than T_c in the entire pseudogap region.^{30,31} Nevertheless our results might signal an upper bound on the length scale for coherent phenomena above T_c . A more specific theoretical framework able to take into account possible effects imposed by “nanosizes” would be necessary for a more complete asset.

The behavior at larger magnetic fields (300 mT) shows a few unexpected features when compared to existing data on LTS.^{4-6,28} Data for D2 are shown in Fig. 2(a) (the parabolic background was subtracted). Oscillations have an amplitude modulation with at least three nodes before completely disappearing at high fields. This beating pattern results from the mix of two or more frequency components that are related to the inverse of the magnetic field. Fast Fourier transform (FFT) of the pattern shown in Fig. 2(b) yields all frequency components in the data. This procedure was successfully used in Ref. 32 to detect the characteristic periodicity arising from fluxoid quantization in two distinct concentric aluminum rings. In our work, apart from the expected peak matching the fundamental periodicity $\Delta H = \Phi_0 / \pi r_{avg}^2$, we found additional peaks. They occur at the same position for all temperatures. Each FFT peak indicates the existence of a characteristic radius associated with flux quantization. Such a multifrequency behavior is made possible by the size of the ring in relation to the characteristic lengths of HTS. The

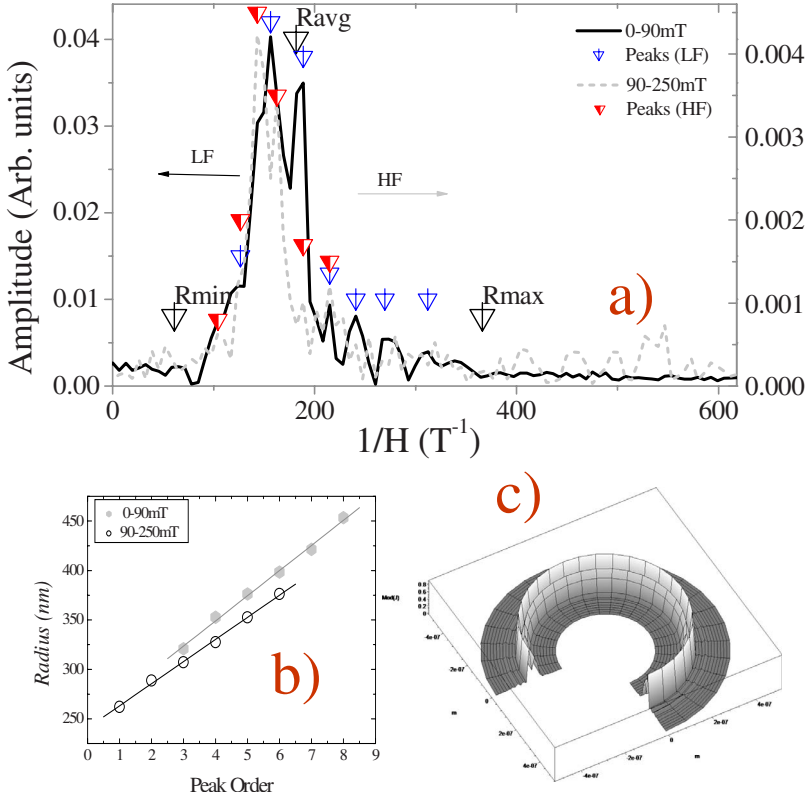


FIG. 3. (Color online) a) FFT of data in Fig. 2(a) in the range 0–90 mT (solid line) and 90–250 mT (dotted line). From the peaks marked in (a) we calculate an effective radius (see text) and plot it as function of peak order (b). In (c) we schematize the concentric vortex structure by plotting, in polar coordinate $\rho = (\Phi_0 H / \pi)^{0.5}$ and θ , the amplitude of the FFT in (a).

“multiple-peak frequency” behavior must be ascribed to the finite width (W) of the ring arms which is here much larger than the superconductor coherence length.

In LTS systems, T_c oscillations were detected in hollow cylinders and rings with walls or arms thinner than ξ . In this case the order parameter can be considered constant along the radial direction and depends only on the azimuthal angle. In the $r \gg \xi$ regime, T_c and other thermodynamic properties, e.g., the magnetization, are strictly $h/2e$ periodic. In HTS systems it is possible to have access to a regime where the radius of the ring is small enough to yield sizable LP oscillations while the width of the arms still supports a significant variation in the order parameter along the radial direction. This sustains a discrete number of concentric independent domains where supercurrent density is different from zero.

III. DISCUSSION

For a superconducting annulus close to T_c with arbitrarily wide arms, Ginzburg-Landau (GL) equations can be used to determine the order parameter (ψ) which, for the cylindrical symmetry of the sample, can be written as $\psi_L(\mathbf{r}) = f_L(\rho)e^{iL\theta}$, where θ and ρ are cylindrical coordinates (origin at the center of the ring). L is called *winding number* or *vorticity* and can be thought of as the angular momentum of the superfluid density. For $W \ll \xi$, $f_L(\rho)$ is a constant, while in our case, $W \gg \xi$, $f_L(\rho)$ varies with ρ .

In our samples the lateral penetration depth exceeds W so that the magnetic field in the structure can be taken equal to the external magnetic field. For the nucleation of superconductivity linearized GL equations can be used^{1,5,6} and the most general solution is a linear combination of states with

different winding number $\psi(r) = \sum a_L \psi_L(r)$.³³ Each $\psi_L(\mathbf{r})$ is characterized by a different average radius and consequently a different periodicity in H . Coefficients a_L must be chosen by minimizing the free energy of the system and maximizing the flatness of ψ (see Ref. 33).

If the external radius $r_o > \pi\xi$, $f_L(\rho)$ has nodes along the radial direction (between the minimum and maximum radius) with an overall spacing $\approx \pi\xi$.³⁴ Consecutive nodes mark concentric domains in which the order parameter and the supercurrent are different from zero.³⁴

A stable solution with lower free energy may take place in a configuration with an order parameter having different vorticity in two domains of a ring separated by a zero-current line rather than the configuration with uniform vorticity.³⁵ In this case the total free energy of the ring will be a sum of contributions from domains with a different periodicity in H .

On the basis of these approaches,^{34,35} we associate each of the peaks in the FFT to the effective radius of one of the elements of a set of concentric current loops populating the ring, each labeled by different superfluid momentum, as schematized in Fig. 3(c), where the FFT is reported in polar coordinates. $R(H)$ data reported in Fig. 2(a) were divided in two groups: from 0 to 90 mT and from 90 to 250 mT: Fig. 3(a) shows the corresponding FFTs (solid and dashed line, respectively). From each of the marked peaks in Fig. 3(a) (g_n) we can calculate a radius value $r_n = (\Phi_0 g_n / \pi)^{0.5}$ that is plotted in Fig. 3(b) as function on the order of the peak. A linear fit of the data yields the average radius spacing Δr at both higher (21 ± 3 nm) and lower (28 ± 2 nm) magnetic field values. From this we can estimate the GL parameter $\xi = \Delta r / \pi = 12 \pm 1$ nm. Finally from this ξ value, by using the

expression for a clean superconductor $\xi_0 = \xi(1 - T/T_c)^{-0.5}$ with $T = 70$ K and $T_c = 74$ K, we obtain $\xi_0 = 1.5 \pm 1$ nm.

The shape of the two FFTs in Fig. 3(a) is rather similar but the one relative to the larger magnetic fields appears somewhat compressed toward zero frequencies. This behavior is in agreement with the theoretical findings of Ref. 36. For a solution of GL equation with fixed vorticity L , the zero current line monotonously shrinks toward the internal radius of the ring with increasing magnetic field.

The multiple-peak structure observed in FFT and the shift of the peaks to lower frequency at higher magnetic field closely resemble what experimentally observed and theoretically expected in Aharonov-Bohm multimode rings in the two-dimensional electron gas.^{37,38} We argue that this striking similarity holds because linearized GL equations, which model our system, are formally identical to the Schrodinger equation which describes single-particle states in a normal ring.¹ The main argument against the hypothesis of a role of quasiparticles interference is the absence of h/e periodicity.¹² Quantitative analyses also rule out explanations of multi-peaked FFT in terms of quasiparticle states with different angular momenta (and radii), as modeled in Ref. 38 for semiconductor multimode rings. In fact, in this case, the differ-

ence between two average radii associated with single-particle states would be of the order $\pi\lambda_F \sim 0.3$ nm, where λ_F is the Fermi wavelength in YBCO (~ 0.1 nm).

IV. CONCLUSIONS

In conclusion we performed LP experiment on several differently doped submicron YBCO rings. Results indicate a multiperiod dependence on H of the free energy close to T_c , consistent with a nonuniform vorticity in the ring. This is a quantum effect due to mesoscopic confinement on HTS nanostructures. We believe these findings can provide useful guidelines for the design of nanoscale experiments targeting the investigation of fundamental properties of HTS.

ACKNOWLEDGMENTS

We acknowledge helpful discussions with J. R. Kirtley, F. Peeters, and V. Moshchalkov. This work has been supported by the MIUR-FIRB Grant No. RBIN06JB4C and EC-STREP “MIDAS-Macroscopic Interference Devices for Atomic and Solid State Physics: Quantum Control of Supercurrents” projects.

¹M. Tinkham, *Introduction to Superconductivity* (McGraw-Hill, New York, 1975).

²Y. Imry, *Introduction to Mesoscopic Physics* (Oxford University Press, New York, 1997).

³Y. Aharonov and D. Bohm, *Phys. Rev.* **115**, 485 (1959).

⁴W. A. Little and R. D. Parks, *Phys. Rev. Lett.* **9**, 9 (1962).

⁵V. V. Moshchalkov, L. Gielen, C. Strunk, R. Jonckheere, X. Qiu, C. Van Haesendonck, and Y. Bruynseraede, *Nature (London)* **373**, 319 (1995).

⁶V. V. Moshchalkov, L. Gielen, M. Dhallé, C. Van Haesendonck, and Y. Bruynseraede, *Nature (London)* **361**, 617 (1993).

⁷A. K. Geim, S. V. Dubonos, J. G. S. Lok, M. Henini, and J. C. Maan, *Nature (London)* **396**, 144 (1998); A. K. Geim, I. V. Grigorieva, S. V. Dubonos, J. G. S. Lok, J. C. Maan, A. E. Filippov, and F. M. Peeters, *ibid.* **390**, 259 (1997).

⁸Y. Liu, Yu. Zadorozhny, M. M. Rosario, B. Y. Rock, P. T. Carrigan, and H. Wang, *Science* **294**, 2332 (2001).

⁹P. Mohanty, J. Y. T. Wei, V. Ananth, P. Morales, and W. Skocpol, *Physica C* **408-410**, 666 (2004).

¹⁰E. W. Carlson, V. J. Emery, S. A. Kivelson, and D. Orgad, in *The Physics of Conventional and Unconventional Superconductors*, edited by K. H. Bennemann and J. B. Ketterson (Springer-Verlag, Berlin, 2002), p. 180.

¹¹J. A. Bonetti, D. S. Caplan, D. J. Van Harlingen, and M. B. Weissman, *Phys. Rev. Lett.* **93**, 087002 (2004); H. A. Mook, P. Dai, and F. Dogan, *ibid.* **88**, 097004 (2002).

¹²F. Loder, A. P. Kampf, T. Kopp, J. Mannhart, C. W. Schneider, and Y. S. Barash, *Nat. Phys.* **4**, 112 (2008); F. Loder, A. P. Kampf, and T. Kopp, *Phys. Rev. B* **78**, 174526 (2008); Y. S. Barash, *Phys. Rev. Lett.* **100**, 177003 (2008).

¹³C. C. Tsuei and J. R. Kirtley, *Rev. Mod. Phys.* **72**, 969 (2000).

¹⁴V. Vakaryuk, *Phys. Rev. Lett.* **101**, 167002 (2008).

¹⁵V. Juricic, I. F. Herbut, and Z. Tesanovic, *Phys. Rev. Lett.* **100**, 187006 (2008).

¹⁶J. C. Wynn, D. A. Bonn, B. W. Gardner, Y.-J. Lin, R. Liang, W. N. Hardy, J. R. Kirtley, and K. A. Moler, *Phys. Rev. Lett.* **87**, 197002 (2001); D. A. Bonn, J. C. Wynn, B. W. Gardner, Y.-J. Lin, R. Liang, W. N. Hardy, J. R. Kirtley, and K. A. Moler, *Nature (London)* **414**, 887 (2001).

¹⁷T. Senthil and M. P. A. Fisher, *Phys. Rev. Lett.* **86**, 292 (2001).

¹⁸T. C. Wei and P. M. Goldbart, *Phys. Rev. B* **77**, 224512 (2008).

¹⁹M. Morelle, D. S. Golubovic, and V. V. Moshchalkov, *Phys. Rev. B* **70**, 144528 (2004).

²⁰V. Bruyndoncx, L. Van Look, M. Verschuere, and V. V. Moshchalkov, *Phys. Rev. B* **60**, 10468 (1999).

²¹P. L. Gammel, P. A. Polakos, C. E. Rice, L. R. Harriott, and D. J. Bishop, *Phys. Rev. B* **41**, 2593 (1990).

²²J. Wei, P. Cadden-Zimansky, and V. Chandrasekhar, *Appl. Phys. Lett.* **92**, 102502 (2008); Yu. Zadorozhny and Y. Liu, *Europhys. Lett.* **55**, 712 (2001).

²³F. Carillo, G. Biasiol, D. Frustaglia, F. Giazotto, L. Sorba, and F. Beltram, *Physica E* **32**, 53 (2006).

²⁴T. T. M. Palstra, B. Batlogg, L. F. Schneemeyer, and J. V. Waszczak, *Phys. Rev. Lett.* **61**, 1662 (1988); R. H. Koch, V. Foglietti, W. J. Gallagher, G. Koren, A. Gupta, and M. P. A. Fisher, *ibid.* **63**, 1511 (1989); H. Safar, L. P. Gammel, D. A. Huse, D. J. Bishop, J. P. Rice, and D. M. Ginsberg, *ibid.* **69**, 824 (1992); W. K. Kwok, S. Fleshler, U. Welp, V. M. Vinokur, J. Downey, G. W. Crabtree, and M. M. Miller, *ibid.* **69**, 3370 (1992).

²⁵P. L. Gammel, L. F. Schneemeyer, J. V. Waszczak, and D. J. Bishop, *Phys. Rev. Lett.* **61**, 1666 (1988); D. J. Bishop, P. L. Gammel, D. A. Huse, and C. A. Murray, *Science* **255**, 165 (1992); P. L. Gammel, *Nature (London)* **411**, 434 (2001).

²⁶M. P. A. Fisher, *Phys. Rev. Lett.* **62**, 1415 (1989); D. R. Nelson

- and H. S. Seung, Phys. Rev. B **39**, 9153 (1989); D. S. Fisher, M. P. A. Fisher, D. A. Huse, *ibid.* **43**, 130 (1991).
- ²⁷V. G. Kogan, J. R. Clem, and R. G. Mints, Phys. Rev. B **69**, 064516 (2004).
- ²⁸R. P. Groff and R. D. Parks, Phys. Rev. **176**, 567 (1968).
- ²⁹D. Y. Vodolazov, D. S. Golubovic, F. M. Peeters, and V. V. Moshchalkov, Phys. Rev. B **76**, 134505 (2007).
- ³⁰For a review, see T. Timusk and B. Stratt, Rep. Prog. Phys. **62**, 61 (1999); Patrick A. Lee, Naota Nagaosa, and Xiao-Gang Wen, Rev. Mod. Phys. **78**, 17 (2006).
- ³¹Y. Wang, L. Li, and N. P. Ong, Phys. Rev. B **73**, 024510 (2006).
- ³²M. Morelle, V. Bruyndoncx, R. Jonckheere, and V. V. Moshchalkov, Phys. Rev. B **64**, 064516 (2001).
- ³³V. V. Moshchalkov, M. Dhallé, and Y. Bruynseraede, Physica C **207**, 307 (1993).
- ³⁴G. Stenuit, J. Govaerts, D. Bertrand, and O. van der Aa, Physica C **332**, 277 (2000).
- ³⁵H. Zhao, V. M. Fomin, J. T. Devreese, and V. V. Moshchalkov, Solid State Commun. **125**, 59 (2003).
- ³⁶S. V. Yampolskii, F. M. Peeters, B. J. Baelus, and H. J. Fink, Phys. Rev. B **64**, 052504 (2001).
- ³⁷J. Liu, W. X. Gao, K. Ismail, K. Y. Lee, J. M. Hong, and S. Washburn, Phys. Rev. B **48**, 15148 (1993).
- ³⁸W.-C. Tan and J. C. Inkson, Phys. Rev. B **53**, 6947 (1996); Semicond. Sci. Technol. **11**, 1635 (1996).